Available online at www.sciencedirect.com

SCIENCE DIRECT®

Bioelectrochemistry 65 (2004) 41–46

Bioelectrochemistry

www.elsevier.com/locate/bioelechem

Direct determination of brucine by square wave voltammetry on 4-amino-2-mercaptopyrimidine self-assembled monolayer gold electrode

Xiu-Hua Zhang, Sheng-Fu Wang*, Ni-Juan Sun

Faculty of Chemistry and Material Science, Hubei University, Wuhan 430062, People's Republic of China

Received 14 July 2003; received in revised form 28 May 2004; accepted 1 June 2004
Available online 7 August 2004

Abstract

4-Amino-2-mercaptopyrimidine self-assembled monolayer (AMP SAMs/Au) was prepared on a gold electrode. The AMP SAMs/Au was characterized by using attenuated total reflection-fourier transform infrared (ATR-FTIR) and A.C. Impedance. The electrochemical behavior of brucine on AMP SAMs/Au was studied by cyclic voltammetry (CV) and square wave adsorptive stripping voltammetry (SWASV). The modified electrode showed an excellent electrocatalytic activity for the redox of brucine. The catalytic current increased linearly with the concentration of brucine in the range of 4.0×10^{-7} to 2.0×10^{-4} mol l^{-1} by square wave voltammetry response. The detection limit was 6.0×10^{-8} mol l^{-1}.

Keywords: Brucine; 4-amino-2mercaptopyrimidine; Self-assembled monolayer (SAMs); Square wave adsorptive stripping voltammetry (SWASV)

1. Introduction

Brucine mainly exists in the seed of *Strychnos nux-vomica*. Its structure is shown in Fig. 1. As an alkaloid, it can be adsorbed by the human body and enter into the blood stream. It has the efficacy of stimulating central nervous system. It is often used as an anti-inflammatory and analgesic drug to relieve arthritic and traumatic pains [1]. Generally, the concentration of brucine in blood is low after metabolization. Thus, the establishment of highly sensitive methods for the determination of brucine is of pharmacological importance. Presently, the determination of brucine is carried out by using UV Spectrophotometry [2], TLC scanning [3] and HPLC [4]. Some electrochemical methods have also been reported for its determination [5–7]. These electrochemical determinations require to pre-oxidize brucine with nitric acid to an ortho-quinone, which can then be reversibly electro- reduced to the corresponding quinol [6,7]. These processes are obviously complex, which will affect the accuracy of determination.

The self-assembled monolayer technique has received much interest in the field of electrochemistry and electroanalytical chemistry during the last decade [8]. In particular, the self-assembly of organosulfur compound on gold surface have been extensively studied. These modified surfaces exhibit new electrochemical and physical properties [9–12].

The aim of this work is to use the short-chain thiol—4-amino-2-mercaptopyrimidine (shown in Fig. 2) to modify the gold electrode. The AMP SAMs/Au was characterized by using attenuated total reflection-fourier transform infrared (ATR-FTIR) and A.C. Impedance. The electrochemical behaviors of brucine at AMP SAMs/Au were investigated. Based on its voltammetric behavior, a square wave adsorptive stripping voltammetry (SWASV) method for the direct determination of brucine was developed. By this method, a detection limit of 8×10^{-8} mol l^{-1} was achieved for the determination of brucine.

2. Experimental

2.1. Apparatus

Electrochemical measurements were carried out with a model CHI660A electrochemical analyzer (CH Instrumen-

* Corresponding author.
E-mail address: wangsf@hubu.edu.cn (S.-F. Wang).

1567-5394/$ - see front matter © 2004 Elsevier B.V. All rights reserved.
doi:10.1016/j.bioelechem.2004.06.001

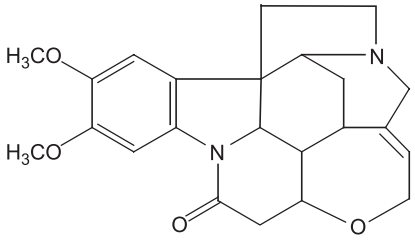

Fig. 1. Chemical structure of brucine.

tal, USA) controlled by a personal computer. A three-electrode system was used in the measurements, with a bare gold electrode (diameter 2 mm) or 4-amino-2-mercapto-pyrimidine (AMP) self-assembled monolayer modified gold electrode (i.e., AMP SAMs/Au) as the working electrode, a saturated calomel electrode (SCE) as the reference electrode and a platinum wire as the auxiliary electrode. Spectrum One FTIR spectrophotometer (Perkin-Elmer, USA) was used to achieve the ATR-FTIR spectra of AMP SAMs/Au at a resolution of 4 cm^{-1} over the 4000–600 cm^{-1} spectral region.

2.2. Chemicals

4-Amino-2-mercapto-pyrimidine was purchased from Aldrich (USA). Brucine was purchased from Sigma (USA). All other chemicals were of analytical-reagent grade. All solutions were prepared with pure water. Brucine is dissolved by K_2SO_4 solution. Then use H_2SO_4 to adjust pH value to 1.0.

2.3. Preparation of the AMP SAMs/Au

Bare gold electrodes were prepared and treated according to Refs. [13,14]. The freshly pretreated electrode was immersed in 10 mmol l^{-1} of 4-amino-2-mercapto-pyrimidine solution for 24 h. The electrodes were ready for use after they were rinsed with pure water and dried under nitrogen atmosphere at room temperature.

3. Results and discussion

3.1. ATR-FTIR characterization of AMP/Au SAMs

Fig. 3 shows the ATR-FTIR spectra of AMP (a) and AMP/Au SAMs (b). Comparing the two spectra, the most important difference is that the stretching vibration band at 2590 cm^{-1} of −SH in Fig. 3a disappeared in Fig. 3b. It is attributed to the cleavage of S−H bond and the formation of a new bond, i.e., S−Au bond. This phenomenon proves that AMP has been assembled on the gold electrode. Furthermore, the vibration bands of $-NH_2$, C−H appeared to exist clearly both in Fig. 3a and Fig. 3b. These facts indicate that the bond of S−Au is strong; other groups in the AMP molecule do not affect its assembling.

3.2. Impedance analysis in the presence of $Fe(CN)_6^{3-/4-}$

The A.C. Impedance method is based upon a measurement of the response of the electrochemical cell to a small-amplitude alternating potential. The response is often shown in the complex-impedance presentation, and the result can be interpreted in terms of an equivalent electrical circuit. The surface changes of the electrode must cause a change in the A.C. Impedance response; this change can be understood according to Randles' equivalent circuit [15], and can be used to estimate the electrode coverage and some kinetic parameter, such as the charge-transfer rate constant, and the dielectric constant of the monolayer film.

In terms of the Randles' equivalent circuit, two frequency regions, as at high and low, can be distinguished to understand the change in faradaic impedance. Our attention is focused on the more interesting part of the spectrum at a high frequency where the electrode reaction is purely kinetically controlled, and the heterogeneous charge-transfer resistance is expected to increase due to inhibition of the electron transfer by the monolayer on the electrode surface [16]. The electrode coverage (θ) is a key factor, which can be used to estimate the surface state of the electrode, and the charge-transfer resistance is also related to it. Assuming that all the current is passed by pinholes on the electrode, the electrode coverage can be calculated by [17]

$$(1-\theta) = R_{ct}^0/R_{ct}, \quad (1)$$

where R_{ct}^0 is the charge-transfer resistance at bare gold and R_{ct} is the charge-transfer resistance at the monolayer-covered electrode under the same conditions.

Fig. 4 is complex-impedance plot of AMP SAMs/Au. A comparison of complex-impedance plots of a bare electrode and a monolayer-covered gold electrode shows the effect of the absorbed AMP monolayers on the A.C. Impedance response. For the monolayer-covered electrode, R_{ct}, which is the diameter of the semicircle at high frequency, is clearly greater than R_{ct}^0 due to an inhibition of AMP SAM to electrode surface. From an analysis of the spectrum shown in Fig. 4, the charge-transfer resistance is 1210 Ω cm^2. The electrode coverage value was estimated to be 99.6%. The charge-transfer resistance for bare gold was measured to be 4.8 Ω cm^2.

3.3. Electrochemical behavior of AMP SAMs/Au

No redox peaks can be observed in cyclic voltammograms of AMP SAMs/Au in the range of 0.7–0.1 V at pH

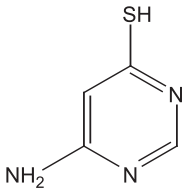

Fig. 2. The structure of 4-amino-2-mercaptopyrimidine.

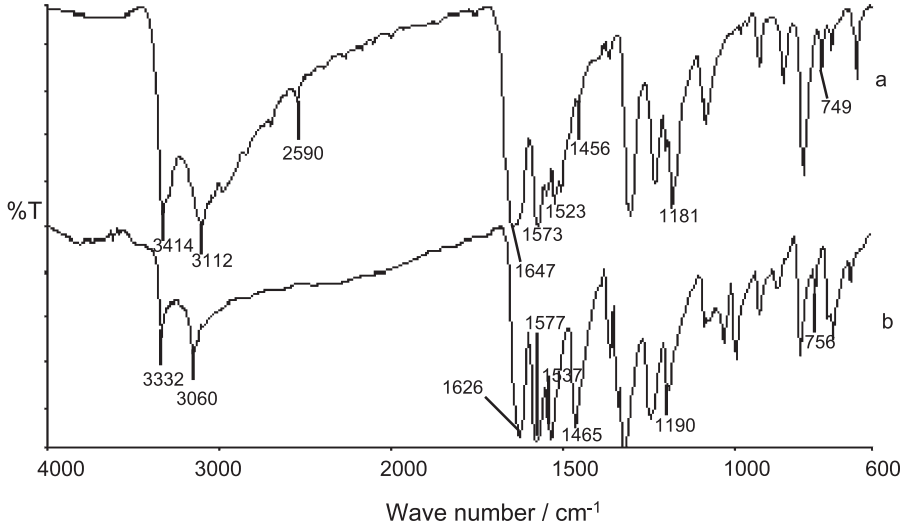

Fig. 3. ATR-FTIR spectra of AMP (a) and AMP/Au SAMs (b).

1.0 electrolyte solution. Compared with bare gold electrode, background current decreased greatly, which indicates that the electrode is efficiently coated by SAMs of AMP and that the AMP monolayer blocks access of solvent molecules and electrolyte ions to the gold surface [18].

Some papers have confirmed that there is a strong affinity between sulfur atom and gold surface, sulfur and selenium compounds can form monolayer on gold [19,20]. Because of containing −SH in 4-amino-2-mercaptopyrimidin molecule, it can be adsorbed on gold electrode naturally, forming self-assembled monolayer.

3.4. Electrochemical properties of brucine at AMP SAMs/Au

As shown in Fig. 5, the Cyclic Voltammetry is used to investigate the mechanism of the redox reaction. The initiative potential is 0.7 V and the scanning potential is between −0.1 and 1.1 V. At the first cathodic scanning, there is no reductive peak. Then at the inverse scanning, only an oxidative peak at the potential of 1.04 V appeared (Fig. 5, I_{pa}). And in the subsequent scanning, a new oxidative peak and a new reductive peak were found, at the potential of 0.517 V (Fig. 5, II_{pa}) and 0.395 V (Fig. 5, II_{pc}), respectively. The currents of II_{pa} and II_{pc} increased with the increase of scanning circles, while the first oxidative peak at 1.04 V (Fig. 5, I_{pa}) tends to decrease.

Fig. 6 shows the SWASV of 1.0×10^{-5} mol l^{-1} brucine on AMP SAMs/Au (a) and the bare gold

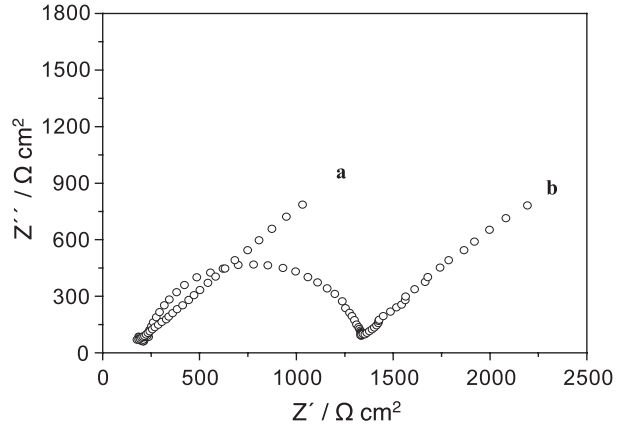

Fig. 4. A.C. Impedance plots in 0.5 mmol/l $[Fe(CN)_6]^{3-}$ + 0.5 mmol/l $[Fe(CN)_6]^{4-}$ + 0.5 mol/l KNO_3 with frequency of $0.05 - 10^5$ Hz for bare gold electrode (a) and AMP SAMs/Au-modified electrode (b).

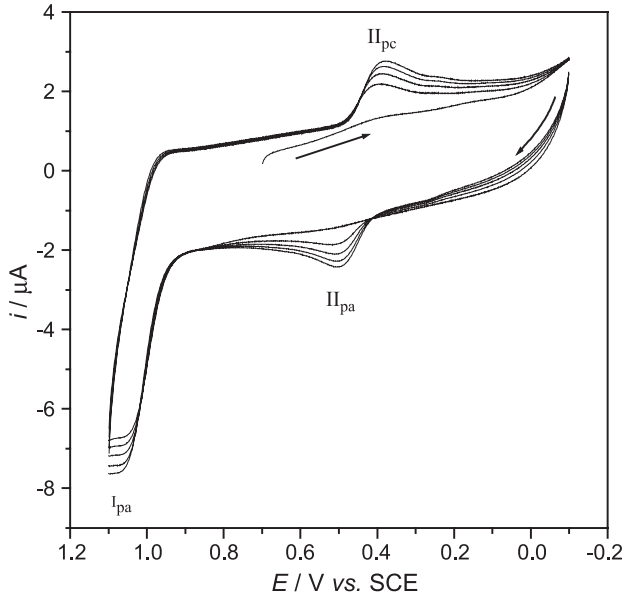

Fig. 5. Cyclic voltammograms of AMP SAMs/Au in 1.0×10^{-4} mol l^{-1} brucine (pH = 1.0) at scan rate of 100 mV/s.

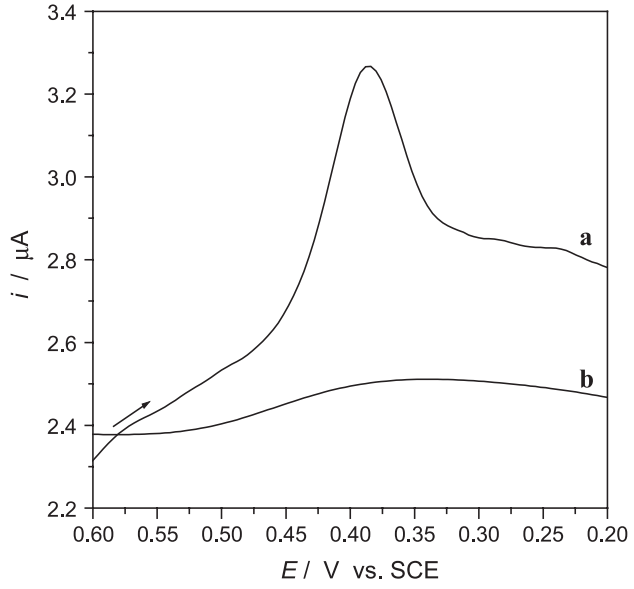

Fig. 6. The SWASV of 1.0×10^{-5} mol l^{-1} brucine on AMP SAMs/Au (a) and on the bare gold electrode (b) at 0.1 mol l^{-1} H_2SO_4 solution.

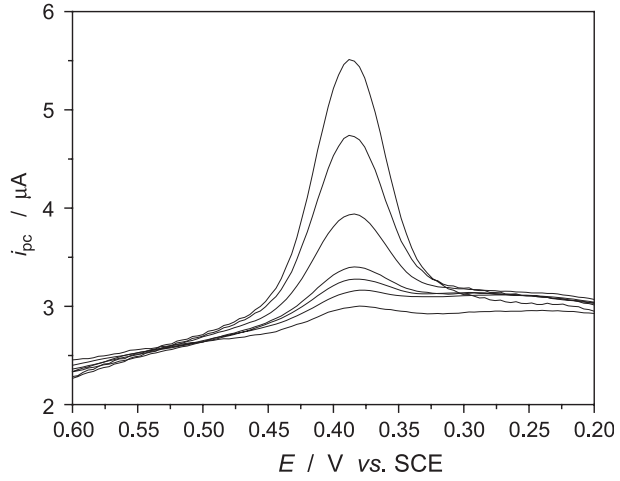

Fig. 8. SWASV of brucine on AMP SAMs/Au at different concentrations (bottom to top): 1.0×10^{-6}, 4.0×10^{-6}, 6.0×10^{-6}, 8.0×10^{-6}, 2.0×10^{-5}, 4.0×10^{-5}, 6.0×10^{-5} mol l^{-1}.

electrode (b) at 0.1 mol l^{-1} H_2SO_4 solution. The reduction peak current of brucine on AMP SAMs/Au was higher than that on bare electrode. The SWASV response of the AMP SAMs/Au electrode to brucine should be ascribed to the interaction between the SAMs of AMP and brucine. The interaction included the electrostatic action [21], which caused the brucine to easily access the surface of AMP SAMs/Au electrode and might result in much faster kinetics of brucine redox [22].

There was a shift in the peak potential when the pH was changed. The potential shifted to lower value as the pH (B.R. buffer) increased according to the equation:

$$E_{pc} = 0.537 - 0.062\text{pH} \quad r = 0.998 \tag{2}$$

A coulometeric study performed in CHI660A electrochemical system showed that the number of the electrons involved in the process, n, was 2. And thus, the proton numbers intervening in the reduction process could also be calculated and found to approximately be 2 from the slope of Eq. (2) [23]. Therefore, the proposed redox mechanism for brucine can be written as Fig. 7 [24,25].

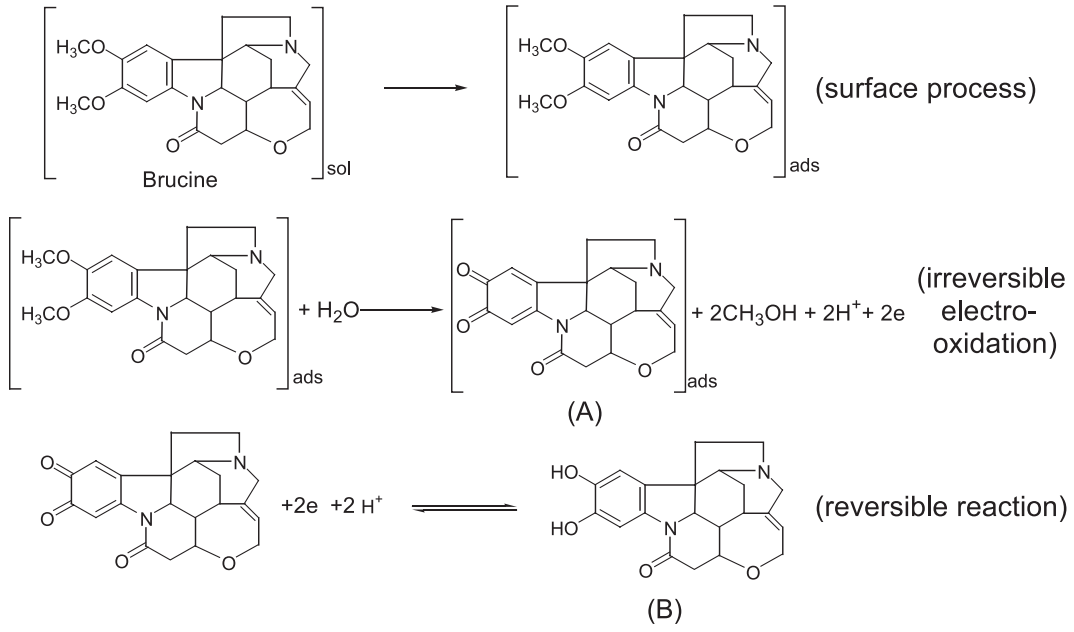

Fig. 7. Redox mechanism of brucine.

Table 1
Determination result of brucine in sample

Sample (μg)	Added (μg)	Sample + Added amount (μg)	Found (μg)	Recovery (%)	Average recovery (%)
	9.33	26.50	27.12	106.6	
	18.66	35.83	36.00	100.9	
	27.99	45.16	45.12	99.9	
17.17	37.32	54.49	54.79	100.8	101.7
	46.65	63.82	64.56	101.6	
	55.98	73.15	72.45	98.7	
	65.31	82.48	84.62	103.3	

Fig. 7 shows the electrocatalytic processes of brucine on the AMP SAMs/Au modified electrode. Firstly, the oxidation of brucine proceeded, after it was absorbed onto AMP SAMs/Au electrode surface. The oxidation production was dicarbonyl-strychnine (Fig. 7A). And then in a reversible electrode reaction, the dicarbonyl-strychnine was reduced to be B.

3.5. Analytical application

The possibility of using the AMP SAMs/Au modified electrode for the determination of brucine was tested. SWASV was adopted in the experiments. The cathodic peak current of 1.0×10^{-6} mol l^{-1} brucine at the AMP SAMs/Au modified electrode increased markedly with preconcentration time up to 300 s at the accumulation potential of 1.04 V. With longer preconcentration time up to 400 s, the rate of the current increase obviously diminished. Considering both sensitivity and time, a time of 300 s was chosen as the preconcentration time. The SWASV parameters that were investigated are the frequency, the pulse amplitude and the pulse increment. These parameters are interrelated and have a combined effect on the current response. The experiment showed the frequency of 30 Hz, the pulse amplitude of 25 mV and the pulse increment of 4 mV were the optimum.

Under the optimum condition chosen, the SWASV peak height was linearly related to the brucine concentration range from 4.0×10^{-7} to 2.0×10^{-4} mol l^{-1}. Fig. 8 shows the SWASV obtained for different concentrations of brucine. The linear regression equation was $i_{pc}(\mu A) = 0.1489 + 0.424c$ ($c/10^{-5}$ mol l^{-1}), with the correlation coefficient of 0.9996. The detection limit was up to 8.0×10^{-8} mol l^{-1}. The relative standard deviation was 1.2% for solution containing 1.0×10^{-5} mol/l brucine ($n = 11$).

In order to evaluate the validity of the proposed method for the determination of brucine in sample, the recovery test was carried out by adding known amounts of brucine standard to sample. As shown in Table 1, the recoveries were from 98.7% to 106.6%, indicating that the method is reliable for the quantification of brucine.

The influence of the interference to 2×10^{-6} mol l^{-1} brucine was evaluated. From the experiment, it is can be conclude that, 500-fold glucose, glutamic acid, uric acid, K^+, Na^+, Ca^{2+}, Al^{3+}, NH_4^+, Cl^-, PO_4^{3-}, SO_4^{2-} and Ac^- did not interfere the determination of brucine, while S^{2-}, Fe^{2+}, NO^{2-}, EP, NE or DA interfered seriously.

4. Conclusion

The performance of the Au electrode coated with a self-assembled monolayer of AMP has been studied. The ATR-FTIR and A.C. Impedance results verified that AMP could be self-assembled spontaneously onto a gold surface through the formation of a S—Au bond. The electrochemical behaviors of brucine on AMP SAMs/Au were studied by cyclic voltammetry and square wave adsorptive stripping voltammetry. The good results obtained in the analysis of content of brucine in sample suggested that the proposed method was suitable for the direct determination of brucine and can be used in routine analysis.

Acknowledgements

The work was supported by Natural Science Foundation of Hubei province of P. R. China (2000J007).

References

[1] T. Yamane, H.A. Mottola, The transient oxidation of brucine in solution as a tool for the determination of chromium(VI) and brucine, Anal. Chim. Acta 146 (1983) 181–190.
[2] Z.P. Kostennikova, UV spectrophotometric determination of strychnine and Brucine in Strychnos nux vomica seeds, Formatsiya 35 (1986) 68–69.
[3] T.M. Ding, Y.P. Zhang, Quantitative determination of brucine, strychnine and ephedrine in rheumatic tablets by TLC-scanning, Chin. J. Pharm. Anal. 13 (1993) 334–338.
[4] Z.P. Gu, S.M. Zhang, C.L. Wang, Determination of strychnine and brucine in strychnos by HPCL, Acta Pharm. Sin. 32 (1997) 791–796.
[5] A.K. Jain, M. Jaham, Tyagiv, construction and assessment of some perchlorate-selective liquid membrane electrodes, Anal. Chim. Acta 231 (1990) 69–75.
[6] M.X. Li, N.F. Hu, Indirect measurement of brucine by adsorptive stripping voltammetry at mercury electrode, Talanta 42 (1995) 1389–1394.
[7] N.X. Wang, X.L. Zhang, Electroanalytical chemistry studies on plant molecular, Journal of Fudan University (Nature Science) 31 (1992) 450–455.
[8] L.H. Dubois, R.G. Nuzzo, Synthesis, structure and properties of model organic surfaces, Annu. Rev. Phys. Chem. 43 (1992) 437–463.
[9] R.C. Retna, K. Tokuda, T. Ohsaka, Electroanalytical applications of cationic self-assembled monolayers: square-wave voltammetric determination of dopamine and ascorbate, Bioelectrochemistry 53 (2001) 183–191.
[10] B. Ge, F. Lisdat, Superoxide sensor based on cytochrome *c* immobilized on mixed-thiol SAM with a new calibration method, Anal. Chim. Acta 454 (2002) 53–64.
[11] Q.J. Wan, N.J. Yang, The direct electrochemistry of folic acid at a 2-mercaptobenzothiazole self-assembled gold electrode, J. Electroanal. Chem. 527 (2002) 131–136.
[12] C.R. Retna, T. Ohsaka, Voltammetric detection of uric acid in the

presence of ascorbic acid at a gold electrode modified with a self-assembled monolayer of heteroaromatic thiol, J. Electroanal. Chem. 540 (2003) 69–77.
[13] S. Bharathi, V. Yegnaraman, G.P. Rao, Potential-dependent ''opening'' and ''closing'' of self-assembled 2-mercaptobenzthiazole on gold substrates, Langmuir 9 (1993) 1614–1617.
[14] C.M. Whelan, M.R. Smyth, C.J. Barnes, The influence of heterocyclic thiols on the electrode position of Cu on Au (III), J. Electroanal. Chem. 441 (1998) 109–129.
[15] M. Sluyters-Rehhach, J.H. Sluyters, in: A.J. Bard (Ed.), Electroanal. Chem. vol. 4, Marcel Dekker, New York, 1970, pp. 1–128.
[16] C. Amatore, J.M. Saveant, D. Tessier, Mechanism analysis of electrochemical reactions involving homogeneous chemical steps: the electrodimerization of 4-methoxybiphenyl, J. Electroanal. Chem. 144 (1983) 59–67.
[17] E. Sabatani, I. Rubinstein, R. Maoz, J. Sagiv, Organized self-assembling monolayers on electrodes: part I. Octadecyl derivatives on gold, J. Electroanal. Chem. 219 (1987) 365–371.
[18] K. Gu, J.J. Zhu, H.Y. Chen, Electrochemical behavior of hemoglobin at a L-cysteine modified microelectrode, Chin. J. Anal. Chem. 27 (1999) 1172–1174.
[19] A. Ulman, Formation and structure of self-assembled monolayers, Chem. Rev. 96 (1996) 1533–1554.
[20] Th. Doneux, Cl. Buess-Herman, J. Lipkowski, Electrochemical and FTIR characterization of the self-assembled monolayer of 2-mercaptobenzimidazole on Au (111), J. Electroanal. Chem. 465 (2004) 65–75.
[21] J.H. Li, G.J. Cheng, S.J. Dong, Applications of self-assembled monolayers in electroanalytical chemistry, Chin. J. Anal. Chem. 21 (1996) 1093–1099.
[22] A. Dalmia, C.C. Liu, R.F. Savinell, Electrochemical behavior of gold electrodes modified with self-assembled monolayers with an acidic end group for selective detection of dopamine, J. Electroanal. Chem. 430 (2001) 205–214.
[23] P. Hernández, I. Sánchez, F. Patón, L. Hernández, Cyclic voltammetry determination of epinephrine with a carbon fiber ultramicroelectrode, Talanta 46 (1998) 985–991.
[24] S.Q. Liu, H.L. Li, M. Jiang, P.B. Li, On the electrochemical oxidation and voltammetric determination of brucine, J. Instrumental Analysis 17 (1998) 5–8.
[25] J.Y. Becker, L.L. Miller, F.R. Stermitz, Electrode processes in the oxidation of tetrahydroisoquinoline derivatives, J. Electroanal. Chem. 68 (1974), 181–189.